SAGE Publishing

Research Article

Experimental Study of the Influence of the Adsorbate Layer Composition on the Wetting of Different Substrates with Water

Michaela Heier [ID],[1] **Rolf Merz** [ID],[2] **Stefan Becker** [ID],[1] **Kai Langenbach** [ID],[1]
Michael Kopnarski [ID],[2] **and Hans Hasse** [ID][1]

[1]*Laboratory of Engineering Thermodynamics, Technische Universität Kaiserslautern, Germany*
[2]*Institute for Surface and Thin Film Analysis, Technische Universität Kaiserslautern, Germany*

Correspondence should be addressed to Hans Hasse; hans.hasse@mv.uni-kl.de

Wetting is strongly influenced by adsorbate layers, which are omnipresent on surfaces. The influence of the composition and thickness of adsorbate layers on the water contact angle of sessile drops on different substrates was systematically investigated in the present work. Measurements were carried out gold-sputtered substrates. These new results are compared to results from a previous study, in which corresponding measurements were carried out for technical steel and titanium substrates. In all experiments, different pretreatments of the samples were used to obtain variations of the adsorbate layer. The samples were either exposed to an oil bath or not, and different cleaning agents were used. The analysis of the adsorbate layer was carried out with X-ray photoelectron spectroscopy (XPS). The results for the different substrates reveal that the water contact angle depends mainly on the composition of the adsorbate layer. The substrate has only an indirect influence, as it influences the composition of the adsorbate layer. The thickness of the adsorbate layers was between 1.4 and 14 nm and was large enough to prevent a direct influence of the substrate on the water contact angle. It is shown that using the information on the adsorbate layer composition from XPS and the results for the water contact angle obtained for the gold samples alone, the water contact angles on the steel and titanium samples can be predicted.

1. Introduction

Wetting of surfaces plays an important role in many processes. It is well known that the wetting is strongly influenced by adsorbate layers on the substrate. Samples without adsorbate layers can only be obtained by special treatments such as plasma cleaning and storage in ultra-high vacuum. Such surfaces have been labeled as *atomically clean* surfaces, in contrast to *technically clean* surfaces [1], which are obtained using conventional cleaning methods and which are always contaminated by residues that form an adsorbate layer. Furthermore, methods for cleaning the surface of contaminants can cause the surface to oxide [2].

Early reports on the influence of adsorbate layers on the wetting were given by Langmuir [3] and Bangham and Razouk [4]. Since then, there has been a continuous interest in the topic, which has been tackled both by experiments as well as by modeling and simulation. However, predicting the influence of adsorbate layers on wetting is still an unsolved problem and there are debates even on fundamental issues: some authors report that contact angles are influenced by the underlying substrate for adsorbate layers with a thickness larger than 10 nm [5–8], while others state that there is no influence of the substrate on the contact angle when the adsorbate layer is thicker than 1-2 nm [8, 9]. The different findings are probably related to the nature of the adsorbate layer. All reports on a long-range influence of the substrate are for adsorbate layers of long-chain molecules, while the authors who did not observe an influence of the substrate on the contact angle for an adsorbate layer thicker than 1-2 nm studied surfaces contaminated with simpler molecules. Their observations are in good agreement with molecular considerations: nonionic interactions fade out quickly with increasing distance of a particle to a surface.

The distance of 1-2 nm corresponds roughly with 5-10 diameters of small molecules, which is enough for nonionic interactions to fade out essentially. The present study focuses on the influence of adsorbate layers on the wetting of technically clean samples. The adsorbate layers on these surfaces are usually thicker than 1-2 nm and do not contain long-chain molecules. The working hypothesis of this study is that for these adsorbate layers, the substrate has no direct influence on the wetting, such that the wetting depends only on the composition of the adsorbate layer.

Fox and Zisman [10] classified solid surfaces into two categories, i.e., high- and low-energy surfaces. The high-energy surfaces include metal, metal oxides, and siliceous gases, whereas the low-energy surfaces consist mainly of organic components [11]. On high-energy surfaces most liquids spread completely, i.e., the contact angle is 0° [12]. For atomically clean gold surfaces, Bernett and Zisman [13] and Schrader [11] observed complete wetting with water. However, high-energy surfaces tend to lower their surface free energy by attracting organic residues. The lowered energy of the surface results from physisorption and chemisorption; it leads to an increase of the contact angle and varies with the sample pretreatment [11]. Surveys of the literature show that reported values for water contact angles on gold surfaces vary between 0° and 95° [14, 15]. Also, more recent results lie in this range: Barriga et al. [16] report a water contact angle of 76° on gold-sputtered surfaces; Feng and Zhao [17] investigated the water contact angle on gold-sputtered polydimethylsiloxane. For the thickest gold layer (10 nm) at a humidity of 31%, they observed water contact angles that varied between 80° shortly after the sputtering and 91° after storing the sample for three days. Canning et al. [18] investigated gold-sputtered surfaces, which were cleaned in water and pristine. The water contact angle on the pristine sample was 84°, while for a sample that was pretreated with water 74° were measured immediately after cleaning. All numbers reported above refer to room temperature.

The composition as well as the thickness of adsorbate layers can be studied experimentally by X-ray photoelectron spectroscopy (XPS). XPS is a surface analytical technique, which yields detailed information on chemical properties of surfaces and therefore on the adsorbed residues [19]. In the present work, XPS surface analysis is combined with measurements of water contact angles in order to establish relations between the adsorbate layer composition and the contact angle. Studies in which contact angle and XPS measurements were combined have already been carried out for low-energy and high-energy surfaces (see, e.g., [20–25]).

The experimental work was carried out for gold-sputtered substrates, which show practically no surface roughness. In the experiments, different pretreatments of the samples were used to obtain variations of the adsorbate layer. The present study is closely connected to a previous study by Becker et al. [20], in which the same procedures were applied to technical steel and titanium samples.

The intrinsic contact angle θ_Y on an ideal homogeneous and plane surface is related to the interfacial free energies
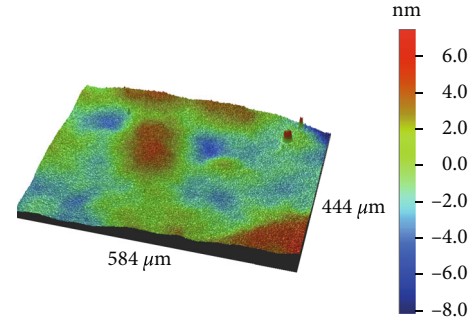

FIGURE 1: Surface topography of a typical gold-sputtered sample studied in the present work. Results from white light interferometry.

by Young's equation [26]:

$$\cos\left(\theta_Y\right) = \frac{\gamma_{sv} - \gamma_{sl}}{\gamma_{lv}}, \tag{1}$$

where "sl" refers to solid-liquid, "sv" to solid-vapor, and "lv" to liquid-vapor. Technical surfaces are neither homogeneous nor plane. The geometric nonideality is usually accounted for by the Wenzel roughness factor r [27]:

$$\cos\left(\theta\right) = r\cos\left(\theta_Y\right), \tag{2}$$

where $\cos\left(\theta\right)$ is the contact angle on the rough surface. The roughness factor r is defined as the ratio between the actual and the projected surface area. While a smooth surface is represented by $r = 1$, a rough surface is represented by $r > 1$. Due to the roughness, the actual contact angle θ increases if $\theta_Y > 90°$ and decreases if $\theta_Y < 90°$.

The present paper is organized as follows: first, the analytical techniques and the experimental procedure are described; then, the results are presented and discussed together with those from Becker et al. [20]. Then, the conclusions are drawn.

2. Experimental

2.1. Materials. The samples studied in the present work were prepared in the Nanostructuring Center (NSC) of Technische Universität Kaiserslautern. Silicon (Si) wafers were sputtered first with a 15 nm layer of chromium (Cr) for better attachment of the subsequent gold (Au) layer with 100 nm. The sputtering process was conducted in an Oerlikon UNI-VEX 450 C. The samples had a size of 10 mm × 20 mm. The arithmetic average roughness was $R_a = 1.64$ nm and the root mean squared roughness $R_q = 2.01$ nm. They were determined by white light interferometer using a Wyko NT3300 optical profiler. Figure 1 shows the surface topography of a typical gold-sputtered sample studied in the present work. From the surface topography, the Wenzel roughness factor r can be estimated by the area ratio S_{dr} as described in more detail by Suh et al. [28]. The evaluation shows that the sputtered surfaces can be considered as perfectly flat, i.e., $r = 1$ at least to the 6th decimal digit.

The oil used in this study is a synthetic poly-alpha-olefin (PAO) obtained from Evonik Industries according to SAE class 0 W 20 based on a blend of two poly-alpha-olefines (PAO4, 18.6 wt.% and PAO6, 65.0 wt.%) and an ester (Plastomoll DNA, 10.0 wt.%). As additive and antioxidant, a solution of multifunctional dispersant viscosity-index improver (Viscoplex® 6-850: dispersant polyalkyl methacrylate (PAMA), 6.4 wt.%) is included; no friction or wear-protection additives are included. The cleaning agents used in this study are two nonreactive solvents: cyclohexane with a purity better than 99.9% (Sigma-Aldrich) and acetone with a purity better than 99.8% (Fisher Scientific). For the sessile drops, ultrapure water (ASTM type I) obtained from a Milli-Q® (Merck) system was used.

2.2. Sample Pretreatment.

The gold-sputtered samples were stored in a desiccator. During transport and storage, the gold samples were put on aluminum foil in a closed casket. Between sputtering and XPS analysis, the samples were always stored at least for one day.

After sputtering, the gold samples have a clean surface. For this reason, some gold samples were analyzed by XPS and water contact angle measurements without any cleaning procedure. These samples are called no-cleaning (NC) samples in the following.

Additional samples were subjected to different cleaning procedures. They are split into two classes: there are "oil samples" that were exposed to an oil bath with the synthetic poly-alpha-olefin before cleaning and "no-oil samples" that were not exposed to that oil bath. The oil samples remained in the oil bath for 10 min and were cleaned immediately after the oil bath with lint-free laboratory tissues and a subsequent cleaning procedure. This cleaning procedure was the same for the oil samples and the no-oil samples and consisted of three steps: each sample was put into a clean Erlenmeyer flask filled with a cleaning agent. The Erlenmeyer flask was put into the ultrasonic bath for 10 min at room temperature. After 10 min, the sample was taken out of the flask and rinsed with the corresponding fresh cleaning agent. This procedure was repeated for three times, always with fresh cleaning agent in the Erlenmeyer flask. After rinsing the sample for the third time with the corresponding fresh cleaning agent, the sample was put vertically on a draining board for drying. The sample was dry after less than one minute. Samples that were cleaned three times with cyclohexane are called "CCC samples" and those that were cleaned with acetone are called "AAA samples" in the following.

To avoid changes in the adsorbate layer on the substrate, the samples were brought in the vacuum of the XPS spectrometer immediately after the cleaning procedure. In the XPS spectrometer's sample entry the samples stayed at a decreased pressure of 10^{-6} mbar typically for about 60 minutes. After this, the samples were transferred to the main chamber of the XPS spectrometer, where the pressure is 10^{-8} mbar. They stayed there for approximately 12 hours meanwhile, the measurement was carried out. A sufficient time span in vacuum is crucial to obtain a stable adsorbate layer and therefore a stable water contact angle, cf. Appendix. It is emphasized that the ultra-high vacuum during the XPS analysis has a strong influence on the adsorbate layer. Volatile, only loosely adsorbed species are removed in the vacuum chamber. This has to be considered in the interpretation of the data. The water contact angle was measured immediately after the XPS analysis in a drop shape analysis system.

2.3. Surface Analysis by X-Ray Photoelectron Spectroscopy.

The analysis of the surface chemistry was done by X-ray photoelectron spectroscopy (XPS) with an Axis Nova surface analysis spectrometer (Kratos Analytical Ltd.). In this system, photoelectrons are released from the sample's surface by monochromatic Al Kα radiation of 1486.6 eV at a working pressure of 10^{-8} mbar and analyzed according their kinetic energy by an electrostatic hemispherical sector analyzer.

Two different XPS measuring modes were used: relative atomic concentrations c_i within the XPS information volume were determined by XPS survey spectra at a high electron analyzer pass energy of 160 eV. Elemental binding states were analyzed using XPS detail spectra with a pass energy of 20 eV and therefore about 8 times higher energy resolution than the XPS survey spectra. The relative atomic concentrations c_i are calculated from the corresponding photoelectron intensity I_i for an element i in the XPS information volume by [29]:

$$c_i = \frac{I_i/s_i}{\sum_j \left(I_j/s_j \right)}, \qquad (3)$$

where $i \in j$ and j are all elements detected in the XPS information volume. In the present work, $j = $ Au, C, and O. Standard sensitivity factors s_j given by the spectrometer supplier were used. The photoelectron intensity I_j is defined as the peak area of the elemental photoelectron peak, described as simple Gaussian/Lorentzian profile line-shape, rising above a background of inelastic scattered electrons, described as Shirley type [30]. The XPS information volume is given by the lateral measuring zone (0.35 mm × 0.70 mm) times the maximum escape depth of the photoelectrons, which is typically about 3-5 nm, depending on their kinetic energy and the material which they have to pass.

The atom number fractions in the adsorbate layer x_i for an element i are calculated by omitting the underlying substrate. This is in contrast to the relative atomic concentrations, which refer to the XPS information volume and contain information about the adsorbate layer and the underlying substrate. The atom number fraction in the adsorbate layer x_i is given by the following:

$$x_i = \frac{c_i}{\sum_k c_k}, \qquad (4)$$

where $i \in k$ and k are all elements of the adsorbate layer.

All measurements were conducted at two different detector angles $\alpha = 30°$ and $\alpha = 90°$, which is the angle between surface and detector. Due to the limited effective path length in the sample, which photoelectrons can pass without significant energy loss, a change of the detector angle provides information on different depth regions of the samples. The maximum information depth is obtained for $\alpha = 90°$ and is
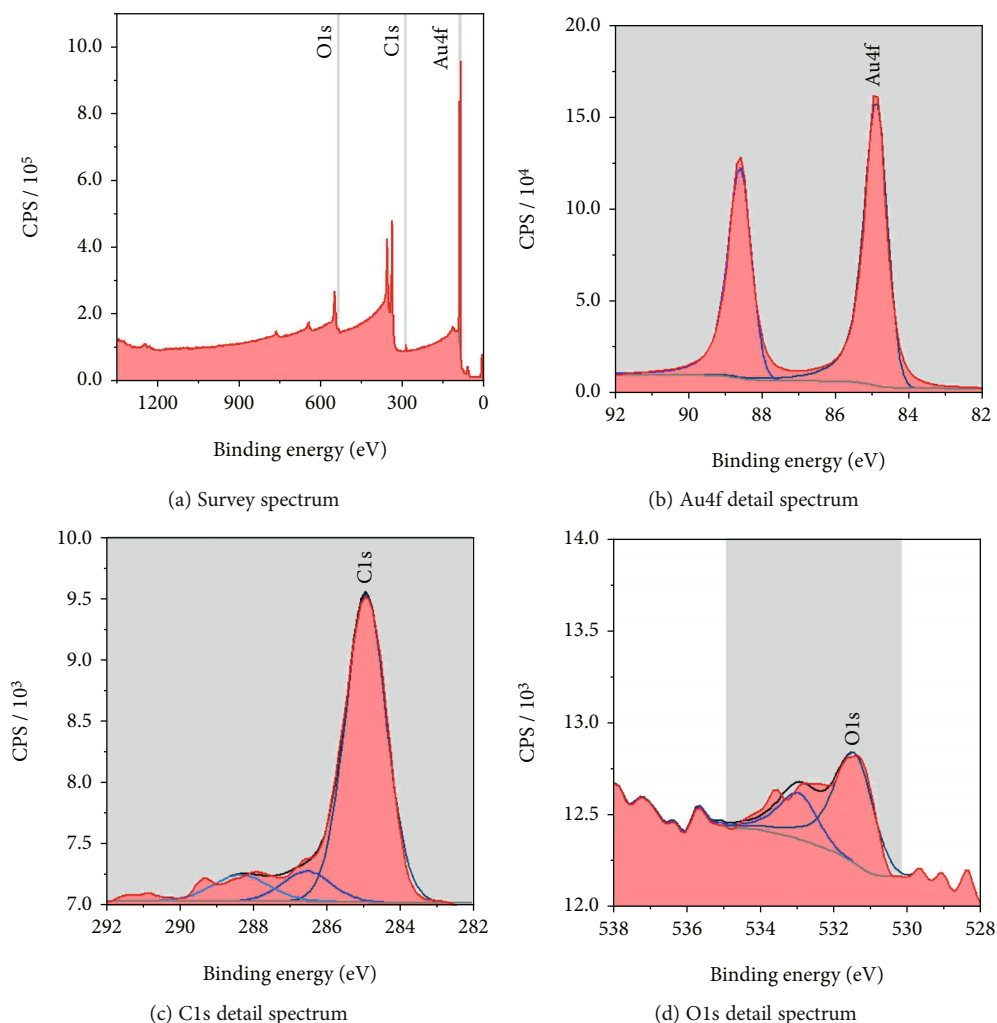
(a) Survey spectrum

(b) Au4f detail spectrum

(c) C1s detail spectrum

(d) O1s detail spectrum

FIGURE 2: XPS survey and detail spectra of a gold-sputtered silicon wafer measured at a detector angle of 90° to the surface, after cleaning three times in a supersonic bath with cyclohexane (CCC sample). Counts per second (CPS) are plotted as function of electron binding energy.

reduced by a factor of $\sin(\alpha)$ by inclining the detector. As an example, Figure 2 shows a set of XPS survey and detail spectra on a CCC no-oil sample by XPS spectroscopy measured at $\alpha = 90°$. In the XPS survey spectrum, it can be seen that only carbon (C), oxygen (O), and gold (Au) are detected. For the example shown in Figure 2, the following relative atomic concentrations were found: $c_C \approx 30$ at%, $c_O < 2$ at%, and $c_{Au} \approx 68$ at %. Hydrogen is not directly detectable by XPS.

Information on the binding states of the detected elements C, O, and Au was obtained from XPS detail spectra, cf. Figure 2 (C1s, O1s, and Au4f regions). The C1s region contains signals from carbon-species in three different binding states: carbon bound in aliphatic and aromatic hydrocarbon at an electron binding energy of 285 eV, carbon with one oxygen as binding partner at 286.6 eV (typical for organic hydroxyl or carbonyl groups), and carbon with two oxygen atoms as binding partners at 288.4 eV (typical for carboxyl groups). In the following, carbon bound in nonpolar aliphatic or aromatic hydrocarbons (signal at 285 eV) is called "nonpolar carbon", with a corresponding atom number frac-

tion in the adsorbate layer of $x_{C^{np}}$. Carbon bound in polar groups with one or two oxygen atoms as binding partners is called "polar carbon", with a corresponding atom number fraction in the adsorbate layer of x_{C^p} (sum of the signals at 286.6 eV and 288.4 eV). The oxygen region of the spectrum contains always at least two signals: they stem from oxygen bound in hydroxyl and carbonyl groups at 531.2 eV-532.3 eV and oxygen bound in carboxyl groups at 532.2 eV-533.6 eV [30]. Only the sum of the signals in the oxygen region is used here as the deconvolution of the peaks is subject to large uncertainties; the corresponding atom number fraction in the adsorbate layer is x_O. Oxygen bound as water would appear also at 533.2 eV, so the presence of adsorbed water films can not be excluded. The Au detail spectrum shows an Au4f doublet of metallic gold. The doublet is split due to spin-orbit coupling without significant contributions of other binding states.

A comparison of photoelectron intensities that were measured at the two different detector angles is given in Figure 3 in form of a contrast diagram. The contrast C_i is
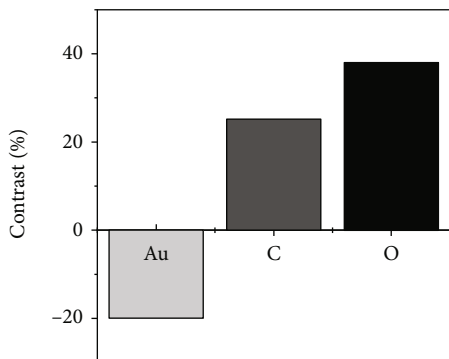
FIGURE 3: Contrast diagram, comparing the Au4f, C1s, and O1s photoelectron intensities measured at 90° and 30° detector angle for a CCC sample. The contrast is defined in Equation (5).

defined as follows:

$$C_i = \frac{I_i(30°) - I_i(90°)}{I_i(30°) + I_i(90°)} \cdot 100\%. \qquad (5)$$

While a contrast of zero would mean that there is no profound depth distribution of the detected elements, a positive contrast indicates an enrichment near the surface, while a negative contrast indicates an enrichment in the deeper regions. Hence, the positive contrast of C and O implies that both are in the adsorbate layer, while the negative contrast of Au is conform with it being the substrate. The strongest positive contrast is detected for O, which implies that O is located even higher than C and that the adsorbate layer has a spatial substructure. Si of the wafer or Cr of the attachment layer under the Au were not detected.

The thickness of the organic layer δ was estimated from the comparison of the attenuation of photoelectron signal intensity of gold Au4f electrons observed upon changing the detector angle from $\alpha = 90°$ to $\alpha = 30°$ using [19]:

$$I_{Au}(\alpha) = I_{Au}^0 \cdot e^{-\delta/(\lambda_L \sin(\alpha))}, \qquad (6)$$

where I_{Au}^0 is the intensity of the signal from the homogeneous bulk material and λ_L is the inelastic mean free way path of photoelectrons in a solid polystyrene sample. Different organic compounds like polystyrene, polymethyl methacrylate or polyethylene give a similar inelastic mean free way path; the variation is less than 10% [31]. The solid polystyrene sample is used as a model substance due to its comparable chemistry and density with the investigated aliphatic hydrocarbon adsorbate layer on metal substrates [31]. By relating the intensities for the two detector angles ($\alpha = 30°$ and $\alpha = 90°$), the thickness of the adsorbate layer δ is obtained from:

$$\delta = \lambda_L \ln \frac{I_{Au}(90°)}{I_{Au}(30°)}. \qquad (7)$$

The statistical uncertainty that is reported here for the results of the adsorbate layer thickness and the atom number fractions is the standard deviation obtained from the results of three measurements that were carried out for each sample.

2.4. Contact Angle Measurement. The water contact angles were measured with a Krüss DSA 100 drop shape analysis system. This analysis system consists of a light source and a camera, which records the shadow pictures of the sessile drop. The DSA 100 is equipped with a thermostatted chamber that provides a water-saturated nitrogen atmosphere, such that the droplet does not evaporate. After a steady state in the chamber was reached, a drop with a volume of 5 μl was deposed on the sample. The temperature was 20.5°C ± 0.5°C. The shape of the droplet is monitored with a camera. For evaluation, the tangent fitting method of the instrument's software was used. The water contact angle of the sessile drop is recorded independently at both sides of the droplet and one mean value for the droplet is calculated. On each sample, three or four drops were deposed and measured. Each drop was measured ten times after two, three, four, and five minutes. No variation of the contact angle throughout this measurement duration was observed. During the first two minutes after deposing the droplet, no measurement was carried out to allow the droplet to reach a steady state. From the results of all these measurements on one sample, the mean water contact angle as well as the standard deviation is calculated for each sample.

3. Results

The results of the XPS analysis and the water contact angle measurement are summarized in Table 1.

Two independent runs were carried out for the CCC, AAA, and NC samples that were not exposed to oil. The water contact angles range from 81° to 93° and the adsorbate layer thickness from 1.4 nm to 2.0 nm for all gold sample measurements carried out in the present work. The adsorbate layer consists mostly of nonpolar carbon.

In the following, the results of this work are discussed together with the results of Becker et al. [20] who used the same sample pretreatment as well as the same wetting liquid (water) as in the present work. Becker et al. [20] used not only acetone and cyclohexane as cleaning agents but also isopropyl alcohol and an aqueous solution of hydrogen peroxide. Isopropyl alcohol is a nonreactive polar solvent and gave similar results for the water contact angle and adsorbate layer as acetone. Therefore, we refrained here from additional measurements with isopropyl alcohol. Nevertheless, the results of this work are discussed together with those for isopropyl alcohol from Becker et al. [20]. The samples cleaned with isopropyl alcohol are called "III samples" in the following.

Hydrogen peroxide forms hydroxyl radicals on steel and titanium surfaces and leads to an oxidation of the surface [32, 33]. Additionally, it has a low cleaning power regarding the oil used in the present work and leaves puddles of oil on the samples (cf. Appendix). These puddles lead to a chemical inhomogeneity of the surface and cause the results for the water contact angle and the data on the adsorbate layer to vary strongly. Therefore, no investigations with aqueous

TABLE 1: Water contact angle θ, adsorbate layer thickness δ, and atom number fractions of oxygen x_O, polar carbon x_{C^p}, and nonpolar carbon $x_{C^{np}}$ in the adsorbate layer measured for the differently prepared gold samples. The number in parentheses indicates the statistical uncertainty in the last decimal digit.

Oil exposure	Cleaning agent	θ (°)	δ (nm)	$x_{C^{np}}$	x_{C^p}	x_O
No-oil	AAA	84.6(18)	1.445(17)	0.779(10)	0.156(18)	0.065(12)
		81.1(17)	1.65(5)	0.6992(37)	0.196(5)	0.105(7)
	CCC	89.7(7)	1.70(6)	0.854(13)	0.0989(36)	0.046(8)
		89.8(13)	1.59(7)	0.783(13)	0.135(10)	0.0821(46)
	NC	86.8(13)	1.54(7)	0.8142(41)	0.132(10)	0.053(5)
		91.3(6)	1.64(6)	0.849(15)	0.106(12)	0.046(9)
Oil	AAA	92.9(12)	2.046(43)	0.747(17)	0.122(8)	0.130(14)
	CCC	89.4(12)	1.57(8)	0.631(6)	0.148(12)	0.221(7)

TABLE 2: Results of Becker et al. [20] for the water contact angle θ, adsorbate layer thickness δ, and atom number fractions of oxygen x_O, polar carbon x_{C^p}, and nonpolar carbon $x_{C^{np}}$ in the adsorbate layer measured for the differently prepared technical steel and titanium samples. The statistical uncertainty of the water contact angle is ±5°. No information on the statistical uncertainty of the atom number fractions is available, but it can be assumed that they are similar to those reported in Table 1 as the same methods were used.

Material	Oil exposure	Cleaning agent	θ (°)	δ (nm)	$x_{C^{np}}$	x_{C^p}	x_O
Steel	No-oil	AAA	67	3.7	0.39	0.21	0.40
		CCC	76	4.3	0.47	0.19	0.34
		III	61	3.4	0.31	0.24	0.45
	Oil	AAA	95	14.3	0.77	0.12	0.11
		CCC	78	5.3	0.57	0.18	0.25
		III	92	8.0	0.68	0.14	0.18
Titanium	No-oil	AAA	86	3.6	0.45	0.25	0.30
		CCC	72	3.3	0.41	0.25	0.34
		III	63	3.0	0.33	0.24	0.43
	Oil	AAA	98	10.8	0.74	0.15	0.11
		CCC	74	4.9	0.51	0.22	0.27
		III	103	10.1	0.73	0.15	0.12

solutions of hydrogen peroxide were carried out in the present work. Furthermore, the results of Becker et al. [20] for hydrogen peroxide, which showed a different behavior than the other cleaning agents for the reasons given above, are not used for discussion. Table 2 lists the results of Becker et al. [20] that are used in the present work.

The literature data on the water-wetting of gold surfaces was already discussed in the Introduction. Different treatments of the samples resulted in strongly varying contact angles in these studies; furthermore, no information on the composition of the adsorbate layers is available. They were therefore not included in the present comparison.

3.1. Adsorbate Layer Thickness.
Figure 4 shows the cosine of the Young water contact angle as a function of the adsorbate layer thickness measured for gold, steel, and titanium substrates after the different pretreatments. The adsorbate layers on the gold substrates are much thinner than those on the other two substrates. This could be caused by two effects:

the differences in the substrate material (gold is inert) as well as variations of the roughness (the gold samples were practically ideally flat). The differences in the material are dominant here, as the roughness factor r for the steel and titanium samples was also very close to 1. For the steel and titanium samples, a trend for an increasing water contact angle with increasing adsorbate layer thickness is observed. For layer thicknesses above 8 nm (oil CCC and oil AAA titanium/steel samples), the water contact angle is basically constant. The gold samples, however, do not fit in this trend. For the gold samples, an almost constant adsorbate layer thickness is observed while the contact angle varies considerably. An exposure to an oil bath leads to higher layer thicknesses than without this exposure for all samples, except for the gold sample cleaned with cyclohexane. For this sample, nearly the same layer thickness is observed as for the corresponding no-oil sample. The samples that were exposed to the oil bath and cleaned with acetone or isopropyl alcohol show the highest adsorbate layer thickness of all substrates. This high
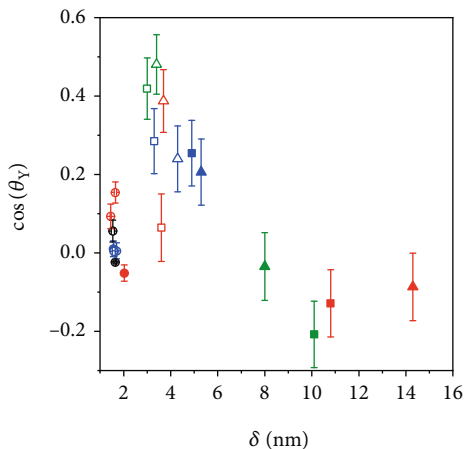
FIGURE 4: Cosine of the water contact angle cos (θ_Y) as function of the adsorbate layer thickness δ. Results for different substrates: gold (circles), steel (triangles), and titanium (squares). Pretreatment: no-oil (open symbols) and with oil (filled symbols). Cleaning: CCC (blue), AAA (red), III (green), and NC (black). The results for gold were obtained in the present work; the other results are taken from Becker et al. [20]. The error bars of the adsorbate layer thickness are within the symbol size.

FIGURE 5: Atom number fractions of oxygen x_O, polar carbon x_{C^p}, and nonpolar carbon $x_{C^{np}}$ in the adsorbate layer. Results for different substrates: gold (circles), steel (triangles), and titanium (squares). Pretreatment: no-oil (open symbols) and with oil (filled symbols). Cleaning: CCC (blue), AAA (red), III (green), and NC (black). The results for gold were obtained in the present work; the other results are taken from Becker et al. [20]. No error bars are depicted for clarity. The one-parametric empirical correlation (Equation (8)) is shown as black line.

adsorbate layer thickness is caused by residues of the nonpolar oil, which are not removed due to the low cleaning power of the polar cleaning agents acetone and isopropyl alcohol.

Different reasons for the variation of the contact angles on the steel and titanium substrates have been discussed by Becker et al. [20]: the variation of the adsorbate layer thickness as well as the variation of the adsorbate layer composition. However, based on their results alone, the different possible reasons could not be discriminated clearly. This is now possible by including the results for gold. The variation of the water contact angle on the gold samples can not be caused by the layer thickness (which hardly varies). Hence, the variation of the contact angle must be caused by the variation of the adsorbate layer composition.

3.2. Adsorbate Layer Composition. The results for the adsorbate layer composition obtained by XPS are shown in a ternary diagram in Figure 5 as a function of the atom number fractions of oxygen, polar carbon, and nonpolar carbon. Surprisingly, despite the vast differences between the substrates and the pretreatment of the samples, the results for the adsorbate layer composition lie almost on a single straight line in Figure 5. A fit yields the following one-parametric empirical relation:

$$x_O = -0.737 x_{C^{np}} + 0.665. \tag{8}$$

The three atom number fractions x_{C^p}, $x_{C^{np}}$, and x_O are related by the summation equation.

The results from the independent measurements for the gold samples that were not exposed to oil (open circles of the same color in Figure 5) enable assessing the experimental error, which is considerably higher than the standard devia-
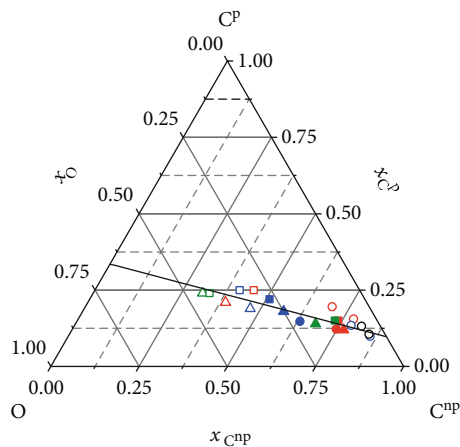
tion of the results obtained on one sample (cf. Table 1). However, the trend described by Equation (8) is confirmed.

The composition of the adsorbate layer on the gold samples (circles in Figure 5) generally shows high concentrations of nonpolar carbon ($x_{C^{np}}$). A tendency is observed comparing the results for the gold samples cleaned with cyclohexane (CCC) with those cleaned with acetone (AAA): cleaning with cyclohexane leads to a slightly higher concentration of nonpolar carbon $x_{C^{np}}$ in the adsorbate layer than cleaning with acetone. This indicates that there are residues of the cleaning agents in the adsorbate layer, despite applying ultra-high vacuum. The gold samples that were not cleaned (NC) show also high values of $x_{C^{np}}$, which leads to the assumption that the gold surface shows an affinity to nonpolar adsorbents. Overall, however, the influence of the cleaning procedure on the adsorbate layer composition is not strong.

The findings for the gold samples that were exposed to an oil bath (full circles in Figure 5) are difficult to interpret. While for the gold sample cleaned with acetone and treated with oil the composition of the adsorbate layer is close to that without an exposure to the oil, this is not the case for the gold samples cleaned with cyclohexane. The adsorbate layer of the gold sample cleaned with cyclohexane that was exposed to oil shows a particularly low concentration of nonpolar carbon. This is completely unexpected. The additives in the oil could possibly lead to polar residues on the sample which could not be removed by cyclohexane. Unfortunately, no independent repetition of that experiment was carried out; we can therefore not exclude an experimental error.

The steel and titanium samples (triangles and squares in Figure 5) have adsorbate layers that contain distinctly more polar groups (x_{C^p} or x_O) than the gold samples (circles). The differences of the composition of the adsorbate layers

on the steel and the titanium substrates are generally not large; they hardly exceed the differences between the replicas of the experiments that were carried out for the gold samples. The most polar cleaning agent, isopropyl alcohol (green symbols in Figure 5), leads to the highest amount of polar groups in the adsorbate layer. This also indicates that residues of the cleaning agents remain in the adsorbate layer on the substrate. However, even when the samples are cleaned with cyclohexane (blue symbols in Figure 5), there are high amounts of polar groups in the adsorbate layer on the steel and titanium samples.

For the steel and titanium substrates, as expected, the amount of nonpolar carbon in the adsorbate layer increases when they are exposed to the nonpolar oil. Interestingly, cleaning with acetone leads to a higher concentration of nonpolar carbon in the adsorbate layer than cleaning with cyclohexane. This is probably due to an ineffective removal of the nonpolar oil by the polar acetone, an interpretation which is supported by the same findings for isopropyl alcohol.

To summarize, the gold surfaces show an affinity to nonpolar adsorbates, whereas the steel and titanium surfaces show an affinity to polar adsorbates. The influence of the cleaning process on the adsorbate layer composition is not dominant, but the results indicate that residues of the cleaning agents are present in the adsorbate layer. Exposing the samples to an oil bath has a strong influence on the adsorbate layer composition for the steel and titanium samples, even after the thorough solvent cleaning in an ultrasonic bath and the exposure of the samples to ultra-high vacuum. Ineffective cleaning of oil with polar solvents leads to increased concentrations of nonpolar carbon in the adsorbate layers for the steel and titanium substrates. The corresponding results for the effect of the oil exposure on the adsorbate layer on gold substrates are inconclusive.

Based on these unexpectedly simple findings for the composition of the adsorbate layer, the hypothesis that the water contact angle depends mainly on the composition was studied in more detail. Figure 5 suggests that the composition of the adsorbate layer can be represented by a single parameter, cf. correlation given in Equation (8). Following the hypothesis of this work, it should also be possible to represent the data on the water contact angle as a function of a single parameter that describes the composition of the adsorbate layer. Different variants of choosing this parameter were tested in a preliminary study and particularly simple results were obtained using the fraction $x_{C^p}/x_{C^{np}}$ as parameter. Figure 6 shows the cosine of the water contact angle $\cos(\theta_Y)$ observed in all experiments that were considered in the present work (cf. Tables 1 and 2) as a function of that parameter. Despite the fact that there are some outliers, a clear trend is visible: $\cos(\theta_Y)$ increases with increasing $x_{C^p}/x_{C^{np}}$. This is not unexpected: increasing $x_{C^p}/x_{C^{np}}$ means that the polarity of the adsorbate layer increases, leading to an increase of the attraction of the polar water and, as a consequence, a decrease of the water contact angle. The straight line shown in Figure 6 is a correlation that was
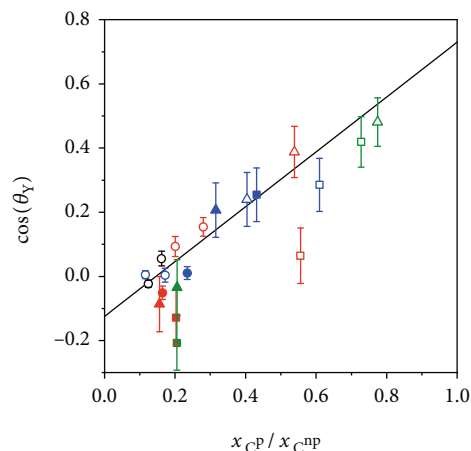

FIGURE 6: Cosine of the water contact angle $\cos(\theta_Y)$ as function of the adsorbate layer composition represented as $x_{C^p}/x_{C^{np}}$. Results for different substrates: gold (circles), steel (triangles), and titanium (squares). Pretreatment: no-oil (open symbols) and with oil (filled symbols). Cleaning: CCC (blue), AAA (red), III (green), and NC (black). The results for gold were measured in the present work; the other results are taken from Becker et al. [20]. The empirical correlation for the water contact angle (Equation (9)) is shown as black line.

obtained from a fit to the results for the gold data in the present work; the steel and titanium data was not used. The line is described by:

$$\cos(\theta_{Y,corr}) = -0.125 + 0.855 \frac{x_{C^p}}{x_{C^{np}}}. \tag{9}$$

Equation (9) does not only represent the gold results well but also gives good predictions for most of the data for the steel and titanium samples. Most of the data shown in Figure 6, including the strongly differing substrates and cleaning procedures, lies within a band of ± 0.1 around $\cos(\theta_{Y,corr})$ (line in Figure 6). There are only three outliers, for which low values of $\cos(\theta_Y)$ were observed (full red and green squares and open red square in Figure 6). All of them are results obtained for titanium substrates cleaned with polar solvents. Two of them were obtained for samples treated with oil (full squares) and show an exceptionally high adsorbate layer thickness (cf. Table 2). It can be speculated that the adsorbate layer on these substrates is inhomogeneous. Furthermore, the roughness of the titanium substrates was larger than that of the other substrates, which can cause the deviations from Equation (9).

4. Conclusions

The working hypothesis of the present study was that for adsorbate layers on technically clean surfaces the substrate has no direct influence on the wetting, such that the wetting depends mainly on the composition of the adsorbate layer. This hypothesis was put to an experimental test and confirmed.

Adsorbate layers on gold-sputtered silicon wafers were analyzed regarding the adsorbate layer thickness and composition using X-ray photoelectron spectroscopy (XPS), and the XPS analysis was combined with water contact angle measurements. To induce variations of the adsorbate layer, the investigated gold samples were pretreated in various ways: some samples were not cleaned after the sputtering; other samples were cleaned with different cleaning agents (acetone and cyclohexane) in an ultrasonic bath—after having been treated in an oil bath or without such a treatment.

Becker et al. [20] have carried out a corresponding study on technical steel and titanium samples, such that the results from the present work and theirs can be compared directly, i.e., a large amount of data on adsorbate layer compositions and water contact angles, which includes data for strongly differing substrates and treatments, is available.

It was found that the adsorbate layer thickness δ on the gold substrates ($1.4 < \delta < 2.0$ nm) is lower than that on the steel and titanium samples ($3.0 < \delta < 14.3$ nm). The exposure of the samples to an oil bath leads for all but the oil gold sample cleaned with cyclohexane to a thicker adsorbate layer, especially for polar cleaning agents like acetone and isopropyl alcohol, which indicates incomplete cleaning. For the gold samples, no dependency of the water contact angle on the adsorbate layer thickness, which is similar for all samples, was found.

The adsorbate layer composition is influenced by the substrate and its treatment. Surprisingly, despite the differences between the substrates and their treatments, the adsorbate layer composition of all samples can be described by a one-parametric empirical correlation. The gold samples show an affinity for nonpolar adsorbents and the steel and titanium samples an affinity for polar adsorbents.

The water contact angle on all substrates was found to be closely related to the composition of the adsorbate layer. As expected, an increase in the polarity of the adsorbate layer leads to a decrease of the water contact angle. This trend was described quantitatively by an empirical correlation obtained for the results of the gold samples in the present work. In a second step, this correlation was applied to predict the data of the steel and titanium samples, which were not included in establishing the correlation. The data for the steel and titanium samples is predicted astonishingly well, using only the information obtained from the gold samples, and despite the simplicity of the empirical approach. No information about the underlying substrate or about the adsorbate layer thickness is used by this correlation.

We do not claim to have found a universal relation between the water contact angle and the adsorbate layer composition. But the results strongly indicate that, in principle, such a relation exists, at least for adsorbate layers as they are found on technical surfaces. The basic message is important: contact angles measured on technical surfaces do not probe the substrate; they probe the adsorbate layer on the substrate. More generally, only the first 1-2 nm of the components below the wet interface are important for typical wetting contacts, leaving apart specially designs such as polymer-grafted surfaces. This does not mean that there is no influence of the substrate, but this influence is only indi-

TABLE 3: Water contact angle θ on the differently prepared gold samples after various times t in vacuum. The number in parentheses indicates the statistical uncertainty in the last decimal digit.

t (h)	AAA	CCC	NC
0	67.0(19)	77.8(12)	75.3(12)
1	73.86(49)	87.2(11)	83.15(46)
6	79.7(30)	86.0(10)	87.5(7)
15	84.0(8)	90.2(9)	89.6(15)
24	88.86(30)	90.2(5)	89.9(11)
48	84.4(9)	89.57(45)	90.6(9)

rect: the substrate influences the adsorbate layer. The adsorbate layer, however, depends not only on the substrate but also on the treatment of the samples.

The previous discussion is based on the assumption that the adsorbate layer is homogenous. The present experimental results indicate that this might not always be a good assumption. Inhomogeneities in the adsorbate layer can be expected as the adsorbate layer is in general a mixture of components of different properties for which the substrate has varying preferences. This must lead to different compositions of the adsorbate layer near the solid substrate and near the wet interface, which determines the contact angle.

The combination of XPS analysis and contact angle measurements, as it was applied here, is very useful for gaining a better understanding of the wetting of technical surfaces. It also holds promise to create a quantitative theory. As a next step towards this goal, it would be interesting to use the methods established here for studying the wetting of surfaces with different liquids. It would also be desirable to gain more detailed information of the composition of the adsorbate layer, including data on the composition in different depths.

Appendix

A. Contact Angle Variation during Storage in Vacuum

The time span that a sample is exposed to vacuum prior to the XPS analysis and contact angle measurements has a crucial influence on the results. It has to be sufficiently long to obtain stable results for the adsorbate layer and the contact angle. In preliminary measurements, the water contact angle θ on gold-sputtered samples cleaned with cyclohexane (CCC), acetone (AAA), or without cleaning (NC) was investigated for various times t the samples spent in vacuum. Therefore, different samples underwent a cleaning procedure with different cleaning agents and stayed in vacuum for various times. No oil bath was used for these samples. The cleaning procedure was the same as in the main article as well as the determination of the contact angle and the standard deviation of each sample. A vacuum chamber of Thermo Scientific with a sliding vane rotary pump (Pfeiffer Vacuum Pascal 2005SD) with 10^{-3} mbar was used. Table 3 and Figure 7 show the results of each differently pretreated sample of these preliminary measurements.
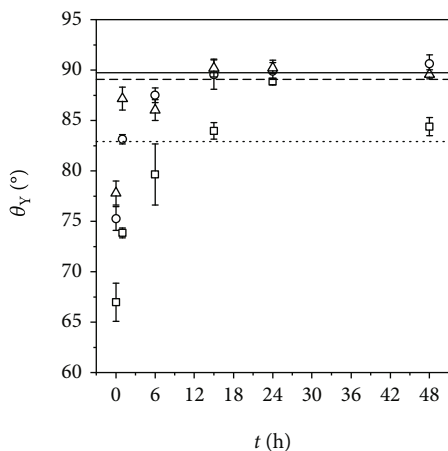
FIGURE 7: Results of the water contact angle measurements θ_Y as a function of the time spent in vacuum after cleaning: CCC (triangle), AAA (square), and NC (circle). The lines are the mean contact angles averaged over the results reported in Table 1 for each cleaning agent: CCC (solid), AAA (dotted), and NC (dashed).

In Figure 7 the results of the preliminary measurements are compared to the mean water contact angle for each cleaning agent ($\bar{\theta}_{AAA} = 82.9°$, $\bar{\theta}_{CCC} = 89.7°$, and $\bar{\theta}_{NC} = 89.1°$), averaged over the two corresponding results of the water contact angle reported in Table 1 in the main article. The results in Figure 7 show that constant contact angles are found if the time the sample has spent in a vacuum of 10^{-3} mbar is longer than 12 hours. If the pressure in the vacuum is decreased, the time the sample has to spent in vacuum is decreased as well.

The result obtained for the gold-sputtered sample that was directly analyzed without any treatment, i.e., the NC sample with $t = 0$ h in vacuum, can be compared to literature data. Barriga et al. [16] reported a water contact angle of 76° on gold-sputtered surfaces without a storage in vacuum. This is in excellent agreement with the result obtained in the present work, cf. Table 3.

These preliminary measurements underline the importance of the sample treatment for the results obtained in the main article of the present work.

B. Cleaning with Hydrogen Peroxide

Becker et al. [20] investigated the water contact angle and adsorbate layer after cleaning with a 30% aqueous solution of hydrogen peroxide. However, the authors of this study did not investigate the wetting on gold substrates with an aqueous solution of hydrogen peroxide due to two reasons: hydrogen peroxide forms hydroxyl radicals at steel and titanium surfaces and leads to an oxidation of the surface [32, 33]. Furthermore, it has a poor cleaning power in regard to the oil used in this work.

In preliminary tests with gold samples a 30% aqueous solution of hydrogen peroxide of VWR chemicals was used as cleaning agent. The cleaning procedure with the aqueous solution of hydrogen peroxide varied slightly from the procedure described in the experimental section of the main part of this article. It still consisted of the three ultrasonic bath steps but instead of rinsing the samples with fresh cleaning agent

after every cleaning in the ultrasonic bath, the samples were rinsed with ultrapure water (ASTM type I). After the three-step ultrasonic cleaning procedure, the samples were put on a heating plate for at least two minutes. The reason for these changes is the slow evaporation of the aqueous solution of hydrogen peroxide which is even slower than the evaporation of ultrapure water.

When cleaning gold oil samples with hydrogen peroxide, small puddles of oil still remained on the samples. In an attempt to remove the remaining oil puddles by wiping with the lint-free tissues, scratches occurred on the surface but still oil puddles remained. These oil puddles and scratches on the sample surface lead to chemically and topographically inhomogeneous surfaces, which cause the water contact angle and the results of the adsorbate layer to vary strongly. Even though the steel and titanium samples are not as soft as gold and do not get scratches as easily as gold, we assume that the oil puddles were also present in the experiments of Becker et al. [20], leading to similar problems as described above. The gold-sputtered samples, however, enable a good observation of such behavior due to their homogeneity. As a consequence of these observations, no investigations with an aqueous solution of hydrogen peroxide were carried out in the main study of the present work.

Data Availability

The contact angle and XPS data used to support the findings of this study are included within the article. Additionally, previously reported contact angle and XPS data were used to support this study and are available at doi:10.1177/0263617416645110. This prior study is cited at relevant places within the text as Becker et al. [20].

Disclosure

Conflicts of Interest

The authors declare that there are no conflicts of interest regarding the publication of this paper.

Acknowledgments

References

[1] K. L. Mittal, "Surface contamination: an overview," in *Surface Contamination: Genesis, Detection, and Control*, K. L. Mittal, Ed., pp. 3–45, Springer US, Boston, MA, USA, 1979.

[2] D. E. King, "Oxidation of gold by ultraviolet light and ozone at 25°C," *Journal of Vacuum Science & Technology A: Vacuum, Surfaces, and Films*, vol. 13, no. 3, pp. 1247–1253, 1995.

[3] I. Langmuir, "The mechanism of the surface phenomena of flotation," *Transactions of the Faraday Society*, vol. 15, pp. 62–74, 1920.

[4] D. H. Bangham and R. I. Razouk, "Adsorption and the wettability of solid surfaces," *Transactions of the Faraday Society*, vol. 33, pp. 1459–1463, 1937.

[5] A. Abbasian, S. R. Ghaffarian, N. Mohammadi, and D. Fallahi, "Sensitivity of surface free energy analysis methods to the contact angle changes attributed to the thickness effect in thin films," *Journal of Applied Polymer Science*, vol. 93, no. 4, pp. 1972–1980, 2004.

[6] C. W. Extrand, "Continuity of very thin polymer films," *Langmuir*, vol. 9, no. 2, pp. 475–480, 1993.

[7] M. Hato, "Attractive forces between surfaces of controlled "hydrophobicity" across water: a possible range of "hydrophobic interactions" between macroscopic hydrophobic surfaces across water," *The Journal of Physical Chemistry*, vol. 100, no. 47, pp. 18530–18538, 1996.

[8] J. Wu and C. M. Mate, "Contact angle measurements of lubricated silicon wafers and hydrogenated carbon overcoats," *Langmuir*, vol. 14, no. 17, pp. 4929–4934, 1998.

[9] W. A. Zisman, "Relation of the equilibrium contact angle to liquid and solid constitution," in *Contact Angle, Wettability, and Adhesion*, F. M. Fowkes, Ed., vol. 43, pp. 1–51, American Chemical Society, Washington, D.C., 1964.

[10] H. W. Fox and W. A. Zisman, "The spreading of liquids on low energy surfaces. I. Polytetrafluoroethylene," *Journal of Colloid Science*, vol. 5, no. 6, pp. 514–531, 1950.

[11] M. E. Schrader, "Ultrahigh-vacuum techniques in the measurement of contact angles. II. Water on gold," *The Journal of Physical Chemistry*, vol. 74, no. 11, pp. 2313–2317, 1970.

[12] P. G. de Gennes, "Wetting: statics and dynamics," *Reviews of Modern Physics*, vol. 57, no. 3, pp. 827–863, 1985.

[13] M. K. Bernett and W. A. Zisman, "Confirmation of spontaneous spreading by water on pure gold," *The Journal of Physical Chemistry*, vol. 74, no. 11, pp. 2309–2312, 1970.

[14] J. R. Gardner and R. Woods, "The hydrophilic nature of gold and platinum," *Journal of Electroanalytical Chemistry and Interfacial Electrochemistry*, vol. 81, no. 2, pp. 285–290, 1977.

[15] M. Yekta-fard and A. B. Ponter, "Surface treatment and its influence on contact angles of water drops residing on polymers and metals," *Physics and Chemistry of Liquids*, vol. 15, no. 1, pp. 19–30, 1985.

[16] J. Barriga, B. Fernández-Diaz, A. Juarros, S. I.-U. Ahmed, and J. L. Arana, "Microtribological analysis of gold and copper contacts," *Tribology International*, vol. 40, no. 10-12, pp. 1526–1530, 2007.

[17] J. T. Feng and Y. P. Zhao, "Influence of different amount of Au on the wetting behavior of PDMS membrane," *Biomedical Microdevices*, vol. 10, no. 1, pp. 65–72, 2008.

[18] J. Canning, N. Tzoumis, J. K. Beattie, B. C. Gibson, and E. Ilagan, "Water on Au sputtered films," *Chemical Communications*, vol. 50, no. 65, pp. 9172–9175, 2014.

[19] D. Briggs and J. T. Grant, *Surface Analysis by Auger and X-Ray Photoelectron Spectroscopy*, IM Publications, Chichester, West Sussex, UK, 1st edition, 2003.

[20] S. Becker, R. Merz, H. Hasse, and M. Kopnarski, "Solvent cleaning and wettability of technical steel and titanium surfaces," *Adsorption Science & Technology*, vol. 34, no. 4-5, pp. 261–274, 2016.

[21] M. D. Doganci, C. E. Cansoy, I. O. Ucar, H. Y. Erbil, E. Mielczarski, and J. A. Mielczarski, "Combined XPS and contact angle studies of flat and rough ethylene-vinyl acetate copolymer films," *Journal of Applied Polymer Science*, vol. 124, no. 3, pp. 2100–2109, 2012.

[22] H. Y. Erbil, B. Yaşar, Ş. Süzer, and B. M. Baysal, "Surface characterization of the hydroxy-terminated poly(ε-caprolactone)/poly(dimethylsiloxane) triblock copolymers by electron spectroscopy for chemical analysis and contact angle measurements," *Langmuir*, vol. 13, no. 20, pp. 5484–5493, 1997.

[23] J. Lai, B. Sunderland, J. Xue et al., "Study on hydrophilicity of polymer surfaces improved by plasma treatment," *Applied Surface Science*, vol. 252, no. 10, pp. 3375–3379, 2006.

[24] S. Takeda, M. Fukawa, Y. Hayashi, and K. Matsumoto, "Surface OH group governing adsorption properties of metal oxide films," *Thin Solid Films*, vol. 339, no. 1-2, pp. 220–224, 1999.

[25] I. O. Ucar, M. D. Doganci, C. E. Cansoy, H. Y. Erbil, I. Avramova, and S. Suzer, "Combined XPS and contact angle studies of ethylene vinyl acetate and polyvinyl acetate blends," *Applied Surface Science*, vol. 257, no. 22, pp. 9587–9594, 2011.

[26] T. Young, "III. An essay on the cohesion of fluids," *Philosophical Transactions of the Royal Society of London*, vol. 95, pp. 65–87, 1805.

[27] R. N. Wenzel, "Resistance of solid surfaces to wetting by water," *Industrial & Engineering Chemistry*, vol. 28, no. 8, pp. 988–994, 1936.

[28] A. Y. Suh, A. A. Polycarpou, and T. F. Conry, "Detailed surface roughness characterization of engineering surfaces undergoing tribological testing leading to scuffing," *Wear*, vol. 255, no. 1-6, pp. 556–568, 2003.

[29] J. C. Vickerman and I. S. Gilmore, *Surface Analysis: The Principal Techniques*, John Wiley & Sons, Chichester, West Sussex, UK, 2nd edition, 2009.

[30] G. Beamson and D. Briggs, *High Resolution XPS of Organic Polymers: The Scienta ESCA300 Database*, John Wiley and Sons Ltd, New York, 1st edition, 1992.

[31] S. Tanuma, C. J. Powell, and D. R. Penn, "Calculations of electron inelastic mean free paths. V. Data for 14 organic compounds over the 50-2000 eV range," *Surface and Interface Analysis*, vol. 21, no. 3, pp. 165–176, 1994.

[32] P. Tengvall, I. Lundström, L. Sjöqvist, H. Elwing, and L. M. Bjursten, "Titanium-hydrogen peroxide interaction: model studies of the influence of the inflammatory response on titanium implants," *Biomaterials*, vol. 10, no. 3, pp. 166–175, 1989.

[33] S. S. Lin and M. D. Gurol, "Catalytic decomposition of hydrogen peroxide on iron oxide: kinetics, mechanism, and implications," *Environmental Science & Technology*, vol. 32, no. 10, pp. 1417–1423, 1998.